

UC Irvine

UC Irvine Previously Published Works

Title

Tightly coupled tripole conductor pairs as constituents for a planar 2D-isotropic negative refractive index metamaterial

Permalink

<https://escholarship.org/uc/item/9144t284>

Journal

Optics Express, 17(17)

ISSN

1094-4087

Authors

Vallecchi, Andrea
Capolino, Filippo

Publication Date

2009-08-13

DOI

10.1364/OE.17.015216

Copyright Information

This work is made available under the terms of a Creative Commons Attribution License, available at <https://creativecommons.org/licenses/by/4.0/>

Peer reviewed

Tightly coupled tripole conductor pairs as constituents for a planar 2D-isotropic negative refractive index metamaterial

Andrea Vallecchi,^{1,2} and Filippo Capolino^{1,*}

¹ Department of Electrical Engineering and Computer Science, University of California, Irvine CA 92697-2625, USA

² Department of Information Engineering, University of Siena, Via Roma 56, 53100 Siena, Italy
[*f.capolino@uci.edu](mailto:f.capolino@uci.edu)

Abstract: A metamaterial, arranged by stacking layers of planar constituents suitably shaped to be responsive to arbitrarily linearly polarized incident waves is here shown to exhibit 2D-isotropic effective negative refractive index (NRI). The general concept underlying this metamaterial design consists of closely pairing two metallic particles to accomplish, as a result of their tight coupling, both symmetric and antisymmetric resonance modes, whose proper superposition can lead to an effective negative refraction response. The proposed structure is composed by layers of periodically arranged pairs of face coupled loaded tripoles printed on the opposite sides of a single dielectric substrate. Through a comprehensive characterization of the transmission properties of such metamaterial, together with the analysis of its dispersion diagram, conclusive evidence that the medium exhibits effective NRI properties as well as good impedance matching to free space is provided. We also describe some guidelines to design the proposed metamaterial with a prescribed operational frequency bandwidth, dependently on the structure parameters.

©2009 Optical Society of America

OCIS codes: (160.4670) Optical materials; (230.3990) Microstructure devices; (260.5740) Resonance; (999.9999) Metamaterials.

References and links

1. J. B. Pendry, A. J. Holden, D. J. Robbins, and W. J. Stewart, "Magnetism from conductors and enhanced nonlinear phenomena," *IEEE Trans. Microw. Theory Tech.* **47**(11), 2075–2084 (1999).
2. D. R. Smith, W. J. Padilla, D. C. Vier, S. C. Nemat-Nasser, and S. Schultz, "Composite medium with simultaneously negative permeability and permittivity," *Phys. Rev. Lett.* **84**(18), 4184–4187 (2000).
3. V. M. Shalaev, W. Cai, U. K. Chettiar, H.-K. Yuan, A. K. Sarychev, V. P. Drachev, and A. V. Kildishev, "Negative index of refraction in optical metamaterials," *Opt. Lett.* **30**(24), 3356–3358 (2005).
4. J. Zhou, E. N. Economou, T. Koschny, and C. M. Soukoulis, "Unifying approach to left-handed material design," *Opt. Lett.* **31**(24), 3620–3622 (2006).
5. J. Zhou, T. Koschny, L. Zhang, G. Tuttle, and C. M. Soukoulis, "Experimental demonstration of negative index of refraction," *Appl. Phys. Lett.* **88**, 221,103/1–3 (2006).
6. G. Donzelli, A. Vallecchi, F. Capolino, and A. Schuchinsky, "Metamaterial made of paired planar conductors: Particle resonances, phenomena and properties," *Metamaterials (Amst.)* **3**(1), 10–27 (2009).
7. V. A. Podolskiy, A. K. Sarychev, and V. M. Shalaev, "Plasmon modes in metal nanowires and left-handed materials," *J. Nonlinear Opt. Phys.* **11**(1), 65–74 (2002).
8. V. Podolskiy, A. Sarychev, and V. Shalaev, "Plasmon modes and negative refraction in metal nanowire composites," *Opt. Express* **11**(7), 735–745 (2003).
9. G. Shvets, and Y. A. Urzhumov, "Negative index meta-materials based on two-dimensional metallic structures," *J. Opt. A, Pure Appl. Opt.* **8**(4), S122–S130 (2006).
10. V. Lomakin, Y. Fainman, Y. Urzhumov, and G. Shvets, "Doubly negative metamaterials in the near infrared and visible regimes based on thin film nanocomposites," *Opt. Express* **14**(23), 11164–11177 (2006).
11. A. Vallecchi, and F. Capolino, "Metamaterials based on pairs of tightly-coupled scatterers," in *Theory and Phenomena of Metamaterials*, chap. 19 (CRC Press, Boca Raton, FL, 2009).
12. J. C. Vardaxoglou, *Frequency Selective Surfaces: Analysis and Design* (Research Studies Press, New York, 1997).
13. B. A. Munk, *Frequency selective surfaces: Theory and Design* (Wiley, New York, 2000).
14. Th. Koschny, L. Zhang and C. M. Soukoulis, "Isotropic three-dimensional left-handed metamaterials," *Phys. Rev. B* **71**, 121103/1–4 (2005).

15. C. R. Simovski, and H. Sailing, "Frequency range and explicit expressions for negative permittivity and permeability for an isotropic medium formed by a lattice of perfectly conducting omega particles," *Phys. Lett. A* **311**(2-3), 254–263 (2003).
16. N. Wongkasemand, A. Akyurtlu, and K. A. Marx, "Group theory based design of isotropic negative refractive index metamaterials," *Progress in Electromagnetics Research* **63**, 295–310 (2006).
17. A. Grbica, G. V. Eleftheriades, "An isotropic three-dimensional negative-refractive-index transmission-line metamaterial," *J. Appl. Phys.* **98**, 043106/1–5 (2005).
18. M. Zedler, C. Caloz, and P. Russer, "A 3-D isotropic left-handed metamaterial based on the rotated transmission-line matrix (TLM) scheme," *IEEE Trans. Microw. Theory Tech.* **55**(12), 2930–2941 (2007).
19. C. Imhof, and R. Zengerle, "Pairs of metallic crosses as a left-handed metamaterial with improved polarization properties," *Opt. Express* **14**(18), 8257–8262 (2006).
20. L. Markley, and G. V. Eleftheriades, "A negative-refractive-index metamaterial for incident plane waves of arbitrary polarization," *IEEE Antennas Wirel. Propag. Lett.* **6**(11), 28–32 (2007).
21. M. Kafesaki, I. Tsiapa, N. Katsarakis, T. Koschny, C. M. Soukoulis, and E. N. Economou, "Left-handed metamaterials: The fishnet structure and its variations," *Phys. Rev. B* **75**, 235114/1–9 (2007).
22. A. Vallecchi, F. Capolino, and A. Schuchinsky, "2-D isotropic effective negative refractive index metamaterial in planar technology," *IEEE Microwave Wireless Comp. Lett.* **19**(5), 269–271 (2009).
23. K. Aydin, K. Guven, M. Kafesaki, L. Zhang, C. M. Soukoulis, and E. Ozbay, "Experimental observation of true left-handed transmission peaks in metamaterials," *Opt. Lett.* **29**(22), 2623–2625 (2004).
24. X. Chen, T. M. Grzegorzczak, B.-I. Wu, J. Pacheco, and J. A. Kong, "Robust method to retrieve the constitutive effective parameters of metamaterials," *Phys. Rev. E* **70**, 016608/1–7 (2004).
25. C. R. Simovski, "Bloch material parameters of magneto-dielectric metamaterials and the concept of Bloch lattices," *Metamaterials (Amst.)* **1**(2), 62–80 (2007).
26. C. R. Simovski, S.A. Tretyakov, "Local constitutive parameters of metamaterials from an effective-medium perspective," *Phys. Rev. B* **75**, 195111/1–9 (2007).
27. C. R. Simovski, "On the extraction of local material parameters of meta-materials from experimental or simulated data," in *Theory and Phenomena of Metamaterials*, chap. 11 (CRC Press, Boca Raton, FL, 2009).
28. D. Seetharamdo, R. Sauleau, K. Mahdjoubi, and A.C. Tarot, "Effective parameters of resonant negative refractive index metamaterials: Interpretation and validity," *J. Appl. Phys.* **98**, 063505/1–4 (2005).

1. Introduction

The combination of split-ring resonators (SRRs) and continuous wires [1,2] was the original breakthrough to design metamaterials (MMs) exhibiting an effective negative refractive index (NRI) in the microwave range. SRRs and wires provided negative effective magnetic permeability and electric permittivity, respectively, over a common frequency range. However, the arrangement of layers of SRRs and wires is not suitable for infrared and optical frequencies because of the way SRRs must be assembled to couple to the incident magnetic field and related fabrication difficulties. Successively, the operation of MMs has been pushed upward in frequency by using pairs of finite-length metallic rods or strips [3,4], that replaced SRR and wires as constitutive particles of a NRI medium. Moreover, fabrication of SRR and wires is somewhat cumbersome also at microwave frequencies, especially when isotropic applications are targeted, since SRRs should be first printed on a substrate, and then cut and assembled so as to couple to the incident magnetic field, which results in a complex fabrication process that is not fully compatible with planar technology.

The pairs of coupled conductor wires [3,4] exhibit both a magnetic resonance (antisymmetric mode) and an electric resonance (symmetric mode) whose frequencies can be properly tuned by adjusting the wires' length. At both microwave [5,6] and optical frequencies [3] different periodic arrangements of paired metallic wires/strips have been proposed for MMs with NRI properties. The cut-wire pair composites are fully compatible with planar fabrication technology and assembly, in contrast to SRR and continuous wire media. This planar design, based on exploiting the antisymmetric mode in pairs of conducting rods or strips, has been successfully exploited in [3,7–10].

In this paper we show that as a generalization of the concept underlying the operation of cut-wire and strip pairs media, a class of fully printable periodic MMs whose unit cells are designed by pairing two substantially arbitrarily, though suitably shaped, conductors can be conceived. We investigate here a particular shape that deviates from the previously studied pairs of rods. However, analogously to short strip pairs, such configurations of coupled conductors can support both antisymmetric (magnetic) and symmetric (electric) resonance modes, whose interaction, if properly engineered, can reflect in simultaneous negative

permittivity and permeability, and, accordingly, NRI behavior. This approach based on pairing two scatterers of general shape has been described in [11].

In the development of a MM by applying the above concept of pairing in tight coupling particles of general shape one can take inspiration for the choice of the unit cell configuration from the variety of geometries that have been developed in the context of frequency selective surfaces (FSSs). FSSs have been used for decades to address specific electromagnetic responses (like for example Jerusalem crosses, tripoles, etc.) of spatial filters exploiting single-particle and collective resonances [12,13]: simply pairing such kind of structures may constitute the starting point to design a range of metamaterials with enhanced capabilities.

In fact, the use of metallic inclusions with more elaborated geometries than simple pairs of short strips offers the possibility to achieve enhanced control on the particle resonances, that can be independently tuned to the desired frequency by adjusting the shape and dimensions of the metallic inclusions, and can also lead to metamaterial structures with a very reduced (i.e., truly subwavelength) size of the unit cell. Furthermore, the shape of the constituent particles can be optimized to realize isotropic metamaterial structures capable of providing a uniform NRI response to arbitrarily polarized incident waves.

Indeed, most of previously designed NIMs are anisotropic, i.e., their properties are polarization dependent; for example, in cut-wire pairs the aforementioned magnetic and electric resonances are only observed for an incident electric field parallel, and magnetic field perpendicular, to the plane containing the two wires. However, it can be foreseen that for many future applications of metamaterials isotropy is desirable. The conditions for 3D-isotropic metamaterials and some proposals, developed either by a crystal-like approach to realize a bulk medium or using loaded transmission lines, can be found in [14–18].

In this paper we present a possible design of a metamaterial whose NRI response is polarization-insensitive, that is, a 2D-isotropic NRI metamaterial, realizable in planar technology. Fully printable NIMs responsive to arbitrary linear incident polarization have been already proposed in [19], as an extension of the cut-wire pair structure, and in [20,21] by modification of the “fishnet” design. A further isotropic structure has been proposed in [22] by pairing two Jerusalem cross conductors.

The proposed new type of 2D-isotropic NRI medium is composed of stacks of periodic arrays of tightly coupled loaded tripole pairs (LTPs) of conductors printed on the opposite sides of a dielectric substrate. Under certain aspects, this arrangement is conceptually linked to the “dogbone” and Jerusalem cross pairs metamaterial [6,22]. Indeed, similarly to these latter structures, a pair of loaded tripoles provides better control of the particle resonances, as compared to the cut-wire pairs and fishnet designs. However, in contrast to the dogbone structure, where the composite medium is sensitive to a single polarization only [6], and somewhat similarly to the Jerusalem cross pairs [22], the proposed metamaterial is demonstrated to exhibit a 2D-isotropic NRI response to arbitrary linearly polarized incident wave. Moreover, with respect to the Jerusalem cross pairs the LTPs allows a further shrinking of the MM unit cell towards a truly subwavelength size. While the tripole geometry has been extensively used in frequency selective surfaces (FSS) [13], it is shown in this work that arrays of pairs of tightly coupled loaded tripoles exhibit a fundamentally different additional property that enables the realization of a new type of 2D-isotropic NRI metamaterials with superior performance. Indeed, the proposed structure features the standard filtering property of FSSs (which is related to the electric resonance [12,13]) and the additional magnetic resonance arising from pairing two extremely close FSSs. We also stress that the resonances are determined by the size and geometry of the single pair, however, because of the proximity of the neighboring pairs, the inter-pair couplings play an important role for both the symmetric and antisymmetric modes. The proposed geometry exhibits stable characteristics when varying polarization and incidence angle of the incoming wave. It is also shown that the substrate losses have negligible impact on the effective medium characteristics provided that the magnetic resonance is reasonably broadband. The additional control of the geometrical parameters, the enhanced design flexibility, and subwavelength size of the constitutive

particles, make this metamaterial an attractive alternative to the SRR-based [2] and fishnet [21] structures, as well as to the paired-rod design [3–10].

2. Metamaterial configuration

The proposed metamaterial, made by stacking the layers shown in Fig. 1, consists of a doubly periodical arrangement of pairs of face-coupled loaded tripole conductors. Such metamaterial provides a 2D-isotropic response to any linearly polarized incident wave because of the symmetry of its constituent cells. The conductor pairs are made of 10- μm -thick copper layers deposited on the opposite sides of a dielectric substrate with permittivity $\epsilon_r = 2.2$ and loss tangent 0.0009, such as commercially available microwave laminates Rogers RT/Duroid 5880 or Taconic TLY-5. The pairs are arranged periodically on a triangular lattice and the resulting hexagonal periodic cell has side length $A = 5$ mm (Fig. 1). In this paper, the thickness H of the dielectric substrate as well as the period C along the stacking z -direction are variable parameters. The default values of the remaining geometrical parameters (Fig. 1(b)) used for the design are $A_1 = 0.722$ mm, $B_2 = 0.5$ mm, $A_2 = 4.885$ mm, and $B_1 = 4$ mm.

The phenomenology of the particle response is somewhat similar to that of the cut-wire or dogbone structures [22], except the polarization sensitivity, and the Jerusalem cross pair one described in [22]. When excited by an incoming plane wave, any orientation (in the x - y plane) of the magnetic field induces a current in the loop formed by the tripole pair central arms and closed by the displacement currents at the external arms (that represent the capacitive loading of the tripoles). These loops, associated with antiparallel currents in the pair of stacked tripoles and opposite sign charges accumulated on the conductors at each end (external arms), give rise to the magnetic resonance, which in turn results in an effective permeability of the patterned layer. The tripole pairs also exhibit an electric resonance due to the excitation of parallel currents in the central stripes and charges of the same sign accumulated by the external arms. This latter resonance can be associated with an effective negative permittivity, and its superposition with the above mentioned magnetic resonance is expected to yield an effective NRI behavior of the composite medium in a certain frequency band.

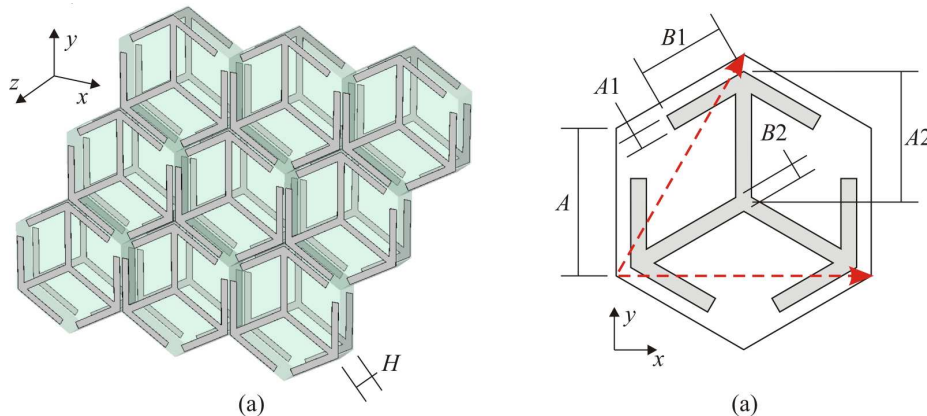


Fig. 1. (a) Perspective view of a layer of the 2D-isotropic metamaterial formed by a periodic arrangement of tightly coupled pairs of loaded tripoles, which exhibit an antisymmetric (magnetic) resonance for any incident linear polarization. (b) Top view of the metamaterial unit cell with geometrical parameters quoted and lattice vectors (dashed). In the simulations, we have set $A = 5$ mm, $A_1 = 0.5$ mm, $B_2 = 0.5$ mm, $A_2 = 4.885$ mm, and $B_1 = 4$ mm.

3. Transmission through a layer of arrayed tripole-pairs: symmetric and antisymmetric modes

Reflection and transmission characteristics of the layer with periodically arranged LTP particles in Fig. 1 have been modeled using a single unit cell with periodical boundary conditions, so that the structure is virtually repeated periodically in the two lattice directions

up to infinity. Specifically, for the triangular lattice considered here, the angle between the lattice vectors is 60 degrees, as shown in Fig. 1(b) where a pair of lattice vectors is drawn in dashed red lines. Simulations have been carried out with the commercial software CST Microwave Studio (CST MWS) and the results have been compared with those obtained by Ansoft HFSS. The data obtained with these two packages, which employ completely different methods, are in very good agreement (cf. Figure 2), and this constitutes a validation of the presented results.

At first, in the numerical analysis we have considered the case of a normally incident plane wave with the electric field polarized along the y -direction. The effect of tilting the plane wave incidence angles is considered subsequently, taking into account both transverse electric (TE) and transverse magnetic (TM) polarizations, with respect to the longitudinal z -direction

Magnitudes of the transmission coefficient $|T|$ at normal incidence for three different values of H ($H = 1, 2, 3$ mm) are shown in Fig. 2(a) for both the cases of lossless and lossy structures. Resonance transmission peaks can be observed that, similarly to those in the dogbone-pair medium [6,11,22], are attributed to a magnetic type resonance. As apparent, for thicker substrates the transmission resonance occurs at lower frequencies and its bandwidth increases. Here we emphasize that the peak is due to the interaction of a narrow band phenomenon (i.e. the magnetic resonance) and the wider band electric resonance. Therefore, in general the frequency of the transmission peak is very close to the magnetic resonance, though, rigorously, we should make a distinction between them.

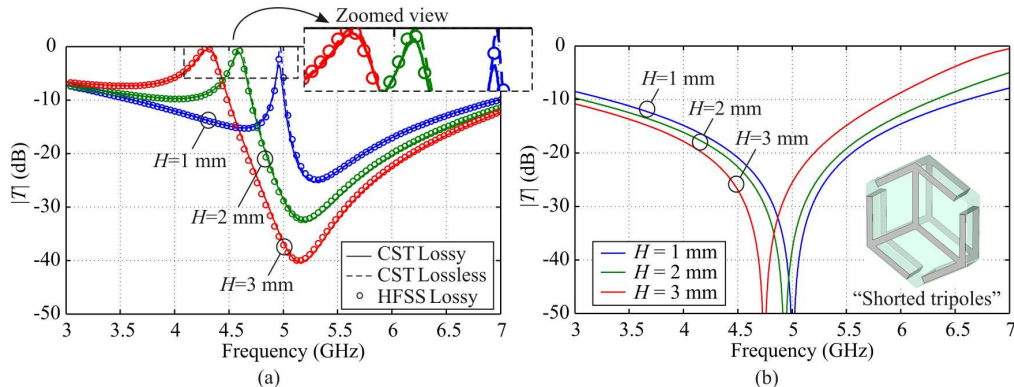


Fig. 2. (a) Simulated transmission coefficients vs. frequency for a layer of periodically arranged LTPs (Fig. 1) at different thicknesses H ($H = 1, 2, 3$ mm) of the dielectric substrate supporting the top and bottom conductors. Solid and dashed lines, almost superimposed, correspond to CST simulations of lossy and lossless structures, respectively; circles represent HFSS results for the respective lossy structure only. (b) LTPs' transmission characteristics when the lateral arms of the tripole particles are short-circuited (see the inset): the magnetic resonance (providing the passband) is suppressed by the short circuits and only the FSS-like stopband electric resonance is present.

To verify the proposed interpretation of the transmission characteristics of a LTP layer, following the method introduced in [23], the same tripole particles have been simulated when their lateral arms were short-circuited (see the inset of Fig. 2(b)). Comparison of the corresponding plots in Fig. 2(a) and Fig. 2(b) shows that no transmission occurs through the tripole structure with the short-circuited arms, and the layer of tripole particles behaves as a standard stopband FSS. This confirms that the transmission peaks in Fig. 2(a) are indeed associated with a resonance of the magnetic type produced by an antisymmetric mode with oppositely directed currents flowing on the top and bottom parts of each tripole pair, since these currents are strongly affected when the arms are short-circuited.

Conversely, the electric resonance is weakly perturbed by the short circuits because it is produced by a symmetric mode whose currents flow in the same direction on both the top and bottom parts of the tripole particle (the only effect on the symmetric mode is a slight decrease

of the electric resonance frequency due to the increased conductor length and capacitance towards neighboring LTPs, provided by the shorting strips).

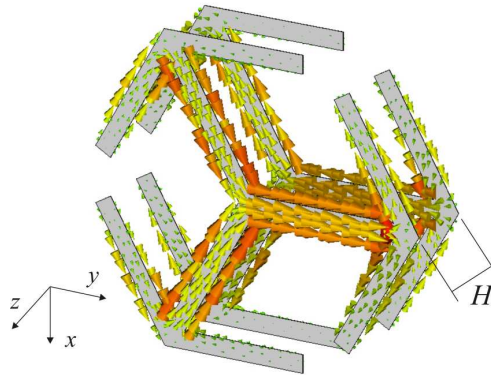


Fig. 3. Antisymmetric surface current distribution on the unit cell of the LTP from Fig. 1 ($H = 2$ mm) calculated by CST MWS at the frequency $f = 4.6$ GHz, near the magnetic resonance f_m . The illuminating plane wave with the horizontally polarized electric field (electric field polarized along the y -axis) is normally incident on the structure from the left-hand side.

Indeed, the surface current distribution on the unit cell of the structure in Fig. 1, with $H = 2$ mm, plotted in Fig. 3 at $f = 4.6$ GHz, near the magnetic resonance f_m , where the peak of transmission occurs (cf. Figure 2(a)), clearly demonstrates that the currents on the two conductors are antisymmetric, and form a sort of loop, which can be represented as an equivalent magnetic dipole moment. This magnetic moment is responsible for the artificial magnetism of the structure, and therefore such a resonance is referred to as a magnetic resonance, similarly to the cases of dogbone pairs and Jerusalem crosses [6,11,22].

It is noted, with reference to Fig. 2(a), that the tripole structures with thinner substrates feature slightly lower levels of transmission and increased attenuation. This is the result of a closer field confinement in the substrate between the conductors that, in turn, causes an increased dissipation of the incident wave by the lossy conductors and dielectric substrate. However, as illustrated in Fig. 2(a), the effect of losses at microwave frequencies is rather insignificant at larger H and does not alter the fundamental features of the LTP characteristics. Therefore, only lossless structures are considered in the remainder of the paper. In the following analyses of transmission through a LTP layer, for reason of conciseness, only results obtained by CST MWS are provided; however, these data have been confirmed by corresponding simulations performed by HFSS. Further comparisons between CST MWS and HFSS results are presented in the analysis of the eigenmode dispersion characteristics of an infinite periodic stack of LTP layers.

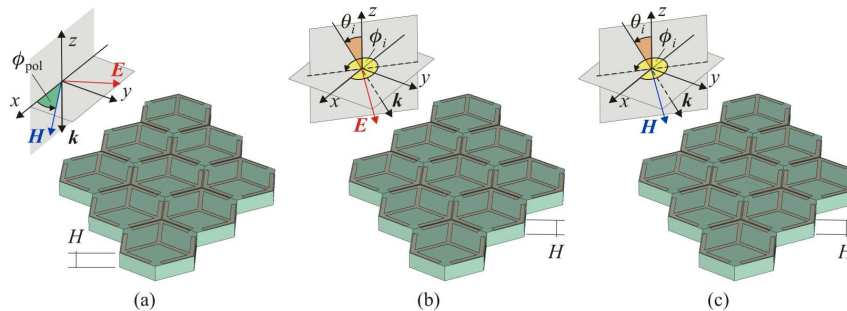


Fig. 4. Simulation setups for: (a) variable polarization at normal incidence; (b) TE (transverse-to- z electric field) obliquely incident plane wave; (c) TM (transverse-to- z magnetic field) obliquely incident plane wave. In (b) and (c) the plane wave is impinging from the direction (θ_i, ϕ_i) .

The unit cell of Fig. 1 was designed with a high degree of symmetry to achieve polarization independence at normal incidence. This property was verified by calculating the response of the metamaterial when the polarization of the incident plane wave is rotated by the angles $\phi_{\text{pol}} = 0^\circ, 30^\circ, 60^\circ, 90^\circ$, as shown in Fig. 4(a). The corresponding transmission coefficients are compared in Fig. 5(a), that shows that the material response should not change for varying incident polarizations.

Furthermore, to evaluate the effect of oblique incidence, the transmission characteristics of the LTP array have been calculated for both TE and TM polarized plane waves impinging onto the array at angles varying from $\theta_i = 0^\circ$ to $\theta_i = 75^\circ$, as shown in Figs. 5(b) and 5(c). (the notation $(\theta_i = 0^\circ, \phi_i = 0^\circ)$ should be intended as a limiting case.) The simulation results in Fig. 5(b) and Fig. 5(c) reveal a remarkable feature of the LTP array, that its transmission resonance frequency is nearly independent of the incidence angle and polarization. Indeed, two different trends can be noticed for the transmission response of the metamaterial at TE and TM polarizations, respectively: in the former case, the transmission resonance peak progressively shrinks at the increasing of θ_i , whereas in the latter the peak slightly moves upward in frequency with θ_i . At any rate, these effects are very limited in a broad range of incidence angles, which implies that the LTP arrays have the potential to provide a NRI response also at oblique incidence.

For the purpose of achieving a comprehensive characterization of the transmission properties of LTPs, in Figs. 5(d) to 5(f) we have also examined the combined effect of either increasingly tilting the incidence angle θ_i of an incoming TE or TM polarized plane wave ($\theta_i = 0^\circ, 15^\circ, 30^\circ, 45^\circ, 60^\circ, 75^\circ$) while ϕ_i is set to 30° (Figs. 5(d) and 5(e)), or making ϕ_i vary ($\phi_i = 0^\circ, 30^\circ, 60^\circ, 90^\circ$) while θ_i is fixed to 30° (Figs. 5(f)). These additional plots confirm the substantial independence of the transmission response of the LTP arrays from the incidence angles and polarization of the incident field.

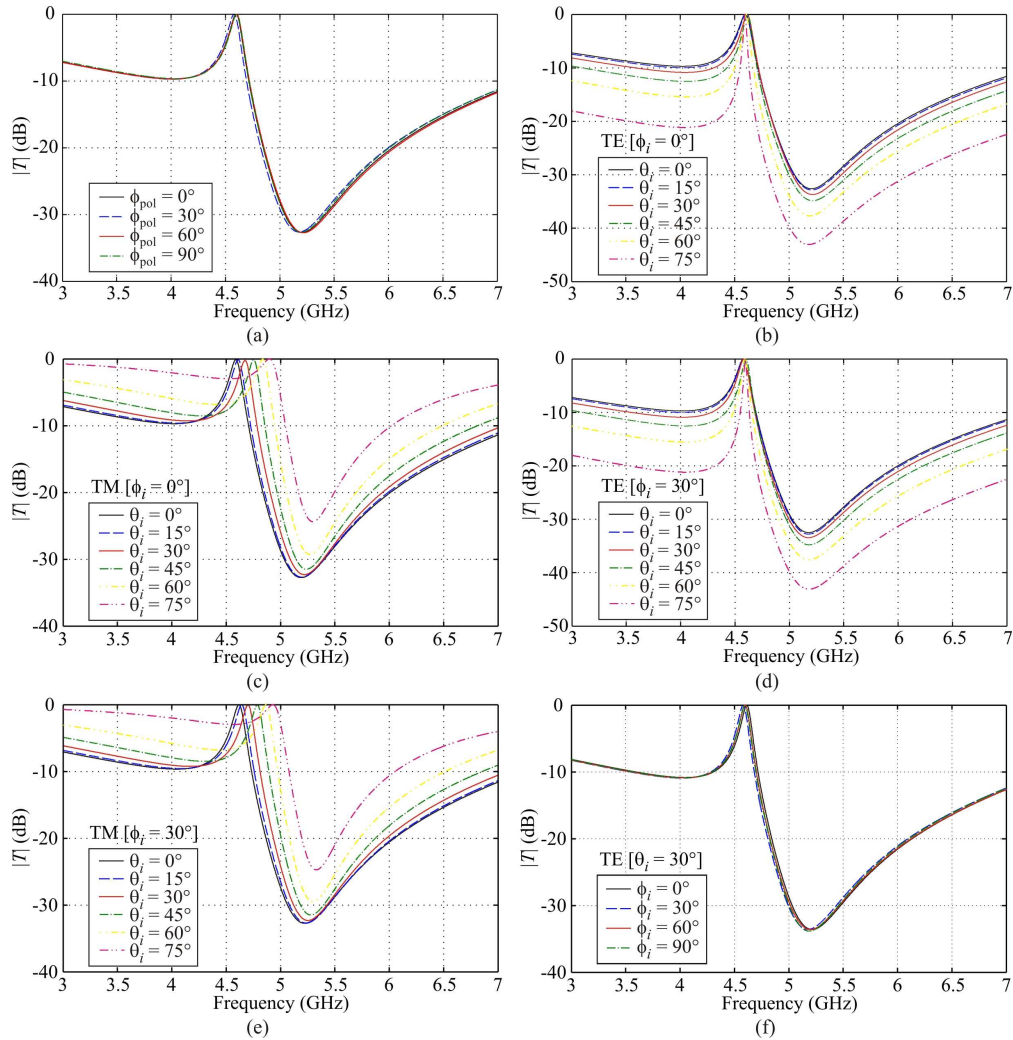


Fig. 5. Simulated (CST MWS) transmission coefficients versus frequency for a layer of periodically arranged LTPs (Fig. 1) with $H = 2$ mm in the different illumination setups displayed in Fig. 4. (a) Normally incident plane waves whose polarization is rotated by the angles $\phi_{\text{pol}} = 0^\circ, 30^\circ, 60^\circ, 90^\circ$; (b) TE plane waves incident at $\phi_i = 0^\circ$ and varying θ_i ; (c) TM plane waves incident at $\phi_i = 0^\circ$ and varying θ_i ; (d) TE plane waves incident at $\phi_i = 30^\circ$ and varying θ_i ; (e) TM plane waves incident at $\phi_i = 30^\circ$ and varying θ_i ; (f) TE plane waves incident at $\phi_i = 0^\circ, 30^\circ, 60^\circ, 90^\circ$ and $\theta_i = 30^\circ$.

4. Left-handed property of the tripole-pairs medium

In order to obtain evidence that the transmission characteristics presented above are associated with a backward-wave phenomenon, we have calculated the effective material parameters in Fig. 6 relative to the structure of Fig. 1 with $C = 6$ mm and $H = 2$ mm, retrieved from the simulated transmission and reflection characteristics for one layer of LTPs at normal incidence. First, following the approach proposed in [24], we have determined the refractive index n and the characteristic impedance Z of an equivalent homogeneous material with thickness C , which are shown in Figs. 6(a) and (b), respectively. Then, from the values of n and Z , the relative permittivity $\epsilon = n/Z$ and permeability $\mu = nZ$ are derived, and their

corresponding plots are displayed in Figs. 6 (c) and (d), respectively. The word “effective” aims at stressing that we refer to the parameters of an equivalent homogenized material.

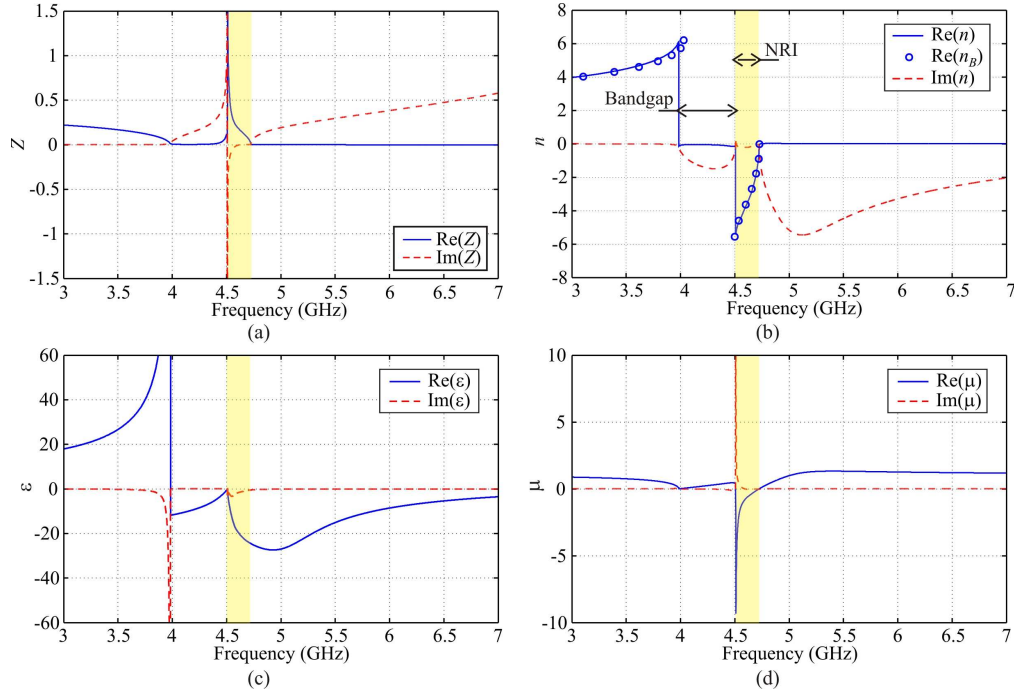


Fig. 6. Effective material parameters for a layer of periodically arranged LTPs (Fig. 1) at normal incidence. The unit cell size along the propagation direction is $C = 6$ mm and the thickness of the dielectric substrate is $H = 2$ mm. The real and imaginary parts of the effective parameters are plotted in solid blue and dashed red lines, respectively. Shaded areas highlight double-negative, i.e. NRI transmission, frequency bands for the considered dielectric substrate thicknesses. (a) Effective impedance; (b) effective refractive index; (c) effective relative permittivity; (d) effective relative permeability.

First, we note from Fig. 6(a) that in the NRI frequency band the normalized effective impedance is real and in the unitary range near the transmission peak frequency for one layer of LTPs. This means that the metamaterial is reasonably well matched to free space, as also observed in the analysis of the transmission properties of a single layer of LTPs (Figs. 2(a) and 5). Moreover, the effective relative permittivity and permeability exhibit the expected resonances and trends, which combine to provide a negative refractive index and good impedance matching to free space. Indeed, the plots show that the real part of the relative permittivity is negative over most of the simulated frequency range (for $f > 4$ GHz). Differently, the real part of the effective relative permeability is negative only over a resonance band that falls within the negative region of ϵ . As a consequence, in the frequency band just above the magnetic resonance the metamaterial presents a double-negative behavior and the extracted real part of the effective refractive index n is found to be negative between 4.5 GHz and 4.75 GHz (Fig. 6(b)). This provides more physical insight into the left-handed nature of the transmission peaks observed in Fig. 2. The NRI band, which is highlighted by a shaded area in Fig. 6, is separated from the relative transmission bands with positive refractive index at low frequencies by a bandgap where transmission is forbidden. The imaginary parts of the effective relative permittivity and permeability are always negative so as to verify the physical constraints [24,27] (we have assumed an $\exp(j\omega t)$ time harmonic dependence), except for a very narrow frequency region slightly above 4.5 GHz. This may be due to numerical inaccuracies in close proximity of the resonance or because the material cannot be homogenized due to the non-negligible contribution of the evanescent modes to the

interference phenomena, as also suggested in [24-28]. However, as shown in the following our results are consistent with the Bloch analysis discussed next.

The existence of an effective NRI band is further verified by analyzing the dispersion characteristics of the eigenmodes in the infinitely extended metamaterial formed by the layers shown in Fig. 1, characterized by the same parameters as in Fig. 2(a) (with $H = 1, 2, 3$ mm), stacked with period C along the z -direction. Figure 7 shows the calculated one-dimensional dispersion diagram versus the Bloch wavenumber k_M along the z direction, normalized with respect to the period $C = 6$ mm; the light line $\omega = k_M c$ (dashed-dotted line), where c is the speed of light and k_0 denotes the free-space wavenumber, is also plotted in Fig. 7 as a reference.

The three branches shown in Fig. 7(a), for each of the different values of H , correspond to the low-frequency region of the dispersion diagram of the lattice made of stacking LTP layers. The lower and upper frequency branches (of the three shown) correspond to the usual low-frequency passband that is split in two portions by the stopband occurring far below the Bragg resonance due to a lattice of electrically resonant scatterers. The narrow passband in the middle arises as a result of the superposition of the electric and magnetic resonances of the tripole particles. Indeed, we have numerically verified that this passband disappears when (i) the lateral arms of the tripole pair are short-circuited (in agreement with results of Fig. 2(b)), and (ii) also when the tripole particle contains only a single conductor. Thus, the middle branches of the dispersion diagram, which are shown in more detail in Fig. 7(b), exist only in the presence of both the magnetic and electric resonances of the tripole particles and represent backward waves with oppositely directed phase and group velocities. In this frequency band the lattice of loaded tripole particles is characterized as a NRI medium. The backward wave propagation for all three thicknesses H of the dielectric substrate supporting the tripole pair conductors is confirmed by the negative slope of the dispersion curves in Fig. 7(b). To corroborate the validity of these results, data obtained by CST MWS are compared with the corresponding ones from HFSS, and, as apparent, the two numerical methods concord on the estimation of the LTP dispersion characteristics (besides their agreement in the prediction of the transmission properties discussed in Sec. 3). These plots also show that for small values of H the NRI passband is narrow, as it can also be inferred from the plots in Fig. 2(a), but a larger NRI band can be achieved at larger H . In fact, larger H values broaden the magnetic resonance and, since this lies within the much broader electric resonance associated with negative effective permittivity, also provides an extended frequency range where permittivity and permeability are both negative. Moreover, it is observed from these results that at larger H the f_m decreases (more precisely, the peak-frequency decreases, however, as we said above, the magnetic resonance is in close proximity of the peak). The illustrative example with $H = 2$ mm shows that predictions of the dispersion characteristics in Fig. 7 are fully consistent with the retrieved refractive index in Fig. 6(b).

In the case of $H = 2$ mm, we have calculated the Bloch effective refractive index as $n_B = k_M c / \omega$, relative to the low-frequency forward propagation and the backward propagation branches shown in Fig. 7(b). This additional result has been added to the plots in Fig. 6(b) and is found to be in good agreement with the effective refractive index obtained by applying to the scattering parameters the retrieval algorithm [24].

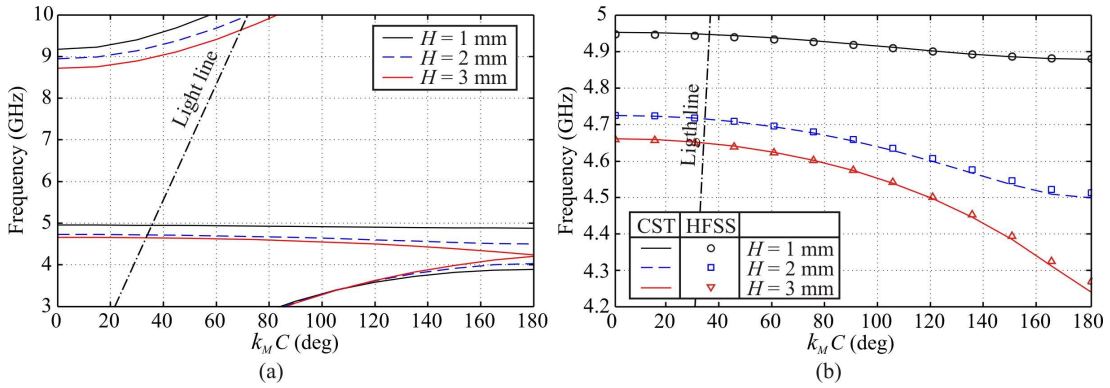


Fig. 7. Dispersion curves for a wave with propagation constant k_M in the infinite periodic metamaterial formed by the LTP structure of Fig. 1 stacked with period $C = 6$ mm along the z -direction at different thicknesses H ($H = 1, 2, 3$ mm) of the dielectric substrate supporting the pairs of conductors. (a) Low-frequency dispersion diagram of the paired tripole lattice as calculated by CST MWS. (b) Enlargement of the NRI passband with comparison of CST MWS (solid black, dashed blue, and solid red lines) and HFSS (circular, square, and triangular markers) results. If the lateral arms of the pair of tripoles would be short circuited, or, in an analogous manner, the tripole pairs in each cell would be replaced by a single tripole conductor, the second passband with negative slope would disappear (cf. Fig. 2(b)).

The dispersion properties of an infinite periodic arrangement of stacked LTP layers have been investigated at several different values of the dielectric spacer thickness H and lattice constant C (along the propagation direction z) to assess the concurrent effects of these parameters on the NRI center frequency, associated to the very close magnetic resonance f_m , and fractional bandwidth $\Delta f / f_m$. These latter characteristics, as retrieved from such dispersion analyses, are plotted in Fig. 8 versus H and at a few values of C . As apparent from Fig. 8(a), f_m (i.e., the transmission band) progressively shifts toward lower frequencies at larger H , it has its lowest values for $H \cong C/2$, and it moves toward higher frequencies for even larger values of H . It is found that $H \cong C/2$ in this case corresponds to the widest NRI bandwidth in addition to the lowest frequency of the magnetic resonance. This is clearly illustrated in Fig. 8(b), which also shows that as long as $H \cong C/2$ the percentage width of the NRI band steadily increases for increasing lengths C of the unit cell in the propagation direction. Furthermore, the plots in Fig. 8(b) show that at the f_m minimum the NRI bandwidth $\Delta f / f_m$ reaches its maximum and can exceed 10%. Thus we can conclude that arrays of tripole pairs with a proper aspect ratio can provide a reasonable bandwidth of NRI performance at low frequencies. Considering the truly subwavelength size of the tripole particles, the presented structure offers new opportunities for the practical realization of homogenizable NRI media. In fact, it is finally important to note that in the NRI frequency band, the ratio of wavelength to the lattice vector length (i.e., $L = A\sqrt{3}$) is of the order of $\lambda / L = 7.5$. Thus, the NRI band should not be confused with the usual high-order Brillouin zones of photonic crystals because the latter do not usually satisfy the $L \ll \lambda$ condition.

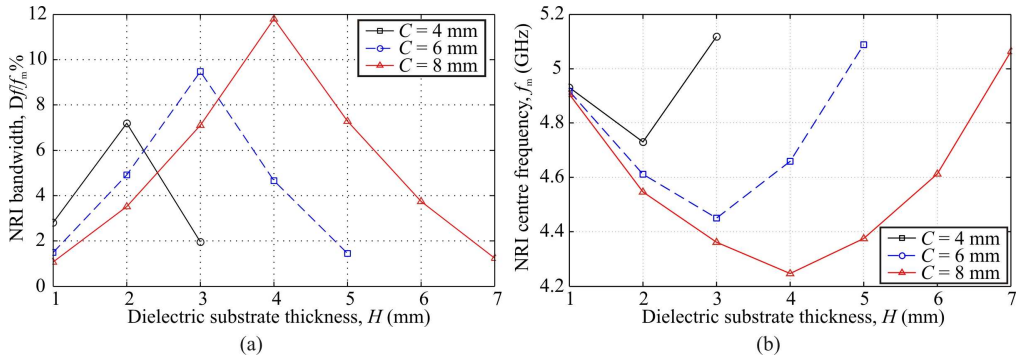


Fig. 8. (a) Center frequency, associated to the very close magnetic resonance f_m , and (b) fractional bandwidth $\Delta f / f_m$ of the backward wave passband vs. thickness H of the dielectric substrate supporting the tripole pairs at a few values of the unit cell size C along the propagation direction as retrieved by CST MWS dispersion analyses.

7. Conclusion

We have illustrated the properties of a metamaterial structure that exhibits a 2D-isotropic negative refractive index (NRI) response and is realized in a fully planar multilayer technology. The metamaterial is 2D isotropic in the sense that the electric field can be arbitrarily polarized in the plane parallel to the metamaterial layer. The proposed metamaterial is composed of a periodic array of tightly coupled loaded tripole conductor pairs printed on the opposite sides of a dielectric substrate. We have demonstrated that the key aspect that each pair supports both symmetric and antisymmetric resonance modes is a general property of tightly coupled layers, and that their superimposition leads to an effective NRI of the composite medium. We have provided evidence that the metamaterial exhibits effective NRI properties for a broad range of structure parameters through a comprehensive characterization of the transmission properties of such metamaterial and also by analyzing the propagation dispersion diagram. The subwavelength size of the constitutive particles and the additional control of the geometrical parameters and enhanced design flexibility make this metamaterial an attractive alternative to the SRRs and wires and fishnet structures. The effect of losses was also investigated at microwave frequencies and it was concluded that dielectric substrate and conductor losses have negligible impact on the effective medium characteristics provided that the magnetic resonance is reasonably broadband.

Acknowledgement

The authors acknowledge Computer Simulation Technology (CST) and Ansoft Corporation for providing their simulation tools that were instrumental in the analysis and design process.